

---

# Orthogonal Curve Analysis of Human Scalp Shapes

Peng Li

US Army DEVCOM SC, Natick, MA 01760, USA

## ABSTRACT

This paper presents a shape analysis on feature curves of 3D bald head scans with the intention of predicting scalp shape under the hair. While there are currently a number of large scale 3D head data collections available around the world, they unfortunately all suffer from hair obstruction preventing an accurate description of true scalp shape. From the 2012 anthropometric survey of US Army personnel (ANSUR II) we have 82 bald head scans from male soldiers available for analysis. This study used these bald head shapes as a basis for exploring the relationship between a small set of head anthropometric measurements and the feature curves of the head. The feature curves include the scalp profile along the sagittal plane, coronal plane and a cross-sectional curve at the level of glabella. Principal component analysis was employed to extract major shape modes of these feature curves and multiple variate linear regression was used to predict scalp shape from a set of head related anthropometric measurements.

**Keywords:** Scalp shape, Anthropometry, 3D head scanning, Principal component analysis, Regression exemplary paper, Human systems integration

## INTRODUCTION

The ever increasing availability of 3D scans of the human head has been a valuable source of information for improving the ability to better describe and understand crania-facial variation as it relates to forensic analysis, plastic surgery, medical diagnosis and face and head-borne protective equipment designs. However, because hair is now well captured in most scanners, it prevents the actual recording and analysis of true scalp shape from 3D scans, and thus the analysis of scalp shape remains an elusive work that is limited to 3D skull data extracted from X-ray or CT scans (Bérar et al., 2006; Lacko et al., 2014). For this reason, much of the data analysis based on 3D head scans is mostly limited on facial shape and some facial landmarks (Goto et al., 2015; Green and Curnoe, 2009; Zhuang et. al., 2010). 3D head/face shape analysis that used 3D scans has been reported (Zhuang et. al., 2013; Liu et al., 2015; Ellena et. al., 2017; Lee et. al., 2017; Dai et. al., 2020) but hair effect cannot be eliminated from the scans. In order to estimate a scalp shape under the hair 3D statistical shape models of a sample set of true scalp shapes have to be created. Lacko et. al. (2015) and Park et. al (2021) have developed PCA regression models of the head to predict scalp shapes from anthropometric measurements, based on data from CT scans and bald head

scans respectively. On the other hand, Paysan et al. (2009) and Bérar et al. (2011) developed statistical models to predict facial shapes from skull data.

In this paper we describe the scalp shape based on a family of orthogonal curves obtained from a small collection of bald head scans. The statistical model of those orthogonal curves was built and multiple linear regression was applied to predict the shape of those curves from a set of anthropometric measurements. In this way, the dimensionality of 3D scalp shape may be reduced and the accuracy of prediction may be improved.

## APPROACH

A total of 82 bald male head scans that met the criteria for inclusion in this analysis were initially identified from the ANSUR II survey database (Gordon et al., 2014). From these bald head scans, we selected three orthogonal feature curves that principally define scalp shape. These curves are profiles along the sagittal plane, the coronal plane and a cross-section at glabella level, as shown in Figure 1. Before acquiring these feature curves, the orientation of a head is normalized by its Frankfort plane. The Frankfort plane is defined by two trignon landmarks and averaged location of two infraorbital landmarks. A head scan is normalized by making its Frankfort plane as the X-Z plane, with the middle point of the trignon-trignon line as the origin of the head, and the X-axis on the trignon-trignon line. As a result, the new head coordinate system has X-axis pointing to the left, Z-axis pointing to the front and Y-axis pointing up. Accordingly, the sagittal plane is the Y-Z plane and coronal plane is the X-Y plane. The feature curves are then sampled in an equal angular space and grouped by their respective plane. In particular, the sagittal and coronal curves start and end on the glabella plane and they are sampled from 0 to 180 degrees. The glabella cross-section is sampled from 0 to 360 degrees.

The collections of each feature curves can be viewed as three separate shape spaces. However, the shapes and dimensions of those three curves are associated to each other in order to define a complete scalp shape. Hence the combined data of the three curves was used in the following analysis. We applied principal component analysis (PCA) to this data set and decomposed the shape variation of the joint curve group into its respective principal axes. As shown in Figure 2, the first four principal components (PC) represent around 90% shape variations and the first six PCs represent around 95% shape variation of this joint shape group. Figure 3 shows the shape variations of the first four PCs with plus and minus three standard deviations from the mean shape, as viewed from the sagittal, glabella and coronal planes. As one may expect the first PC always reflects the overall dimension contrast of the shape group. The rest of PCs shows different shape aspects. Table-1 summarizes the observed shape variation for each PC.

Under PCA decomposition an individual shape is a weighted combination of several PC feature vectors as shown in following formula.

$$S = M + \sum_{i=1}^N w_i * V_i \quad (1)$$

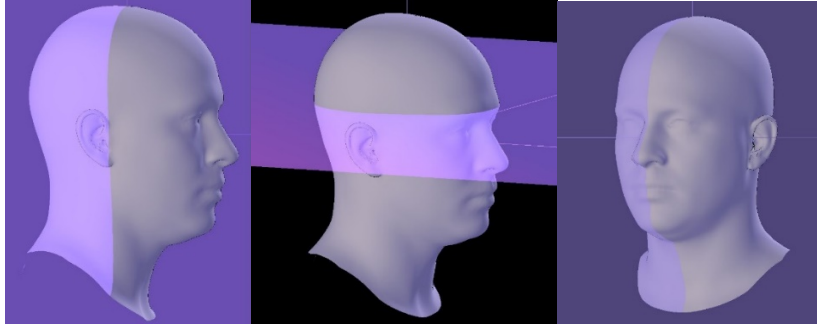


**Figure 1:** Coronal, Glabella and Sagittal sampling plane, after the head orientation is normalized in the Frankfort plane.

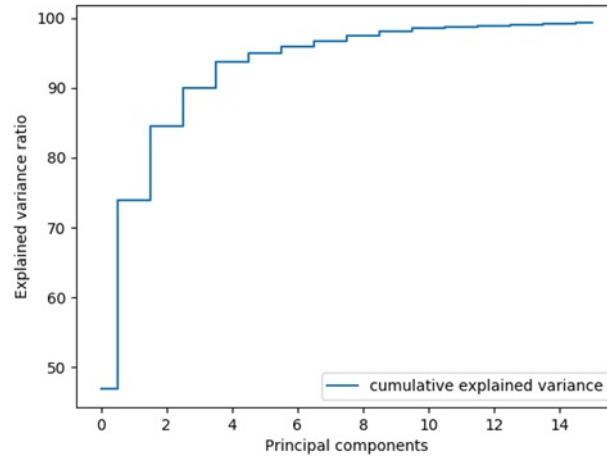


**Figure 2:** The cumulative explained variance of the joint curve PCA.

where  $M$  is the mean shape,  $\{w_i\}$  is the PCA scores (weight) and  $\{V_i\}$  is the loading vectors.

The loading vectors are eigenvectors of PCA that form a shape space. The PCA scores are individual specific values to define a shape. When we have a representative PCA space of cranium curves for a target population we could reconstruct an individual's scalp shape by his/her PCA scores. However, PCA scores are mathematic weights and do not directly associate with an individual's anthropometric measurements that are often the only accessible variables to describe the scalp shapes. Exploring the relationship between the PCA scores and anthropometric measurements will help to predict 3D scalp shape with simple tape and caliper measurements. We hypothesize that a PCA score may be related to the head measurements by a linear equation as shown in formula (2):

$$\tilde{w}_i = a_i + \sum_l b_{li} * m_l \quad (2)$$

where  $m$  is a measurement variable and  $b_{li}$  are regression coefficients.

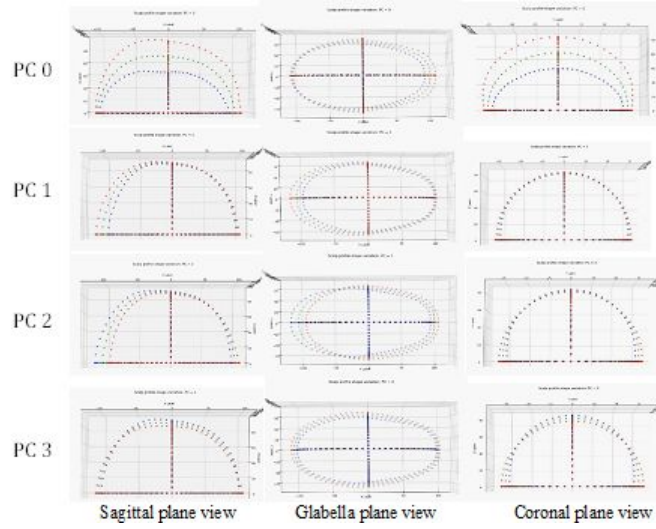


**Figure 3:** PC0 ~ PC3 shape variations of three views of feature curves (mean shape in green, +3SD shape in red, -3SD shape in blue).

So that a predicted scalp shape of orthogonal curves can be expressed as:

$$\tilde{S} = M + \sum_{i=1}^N \tilde{w}_i * V_i = M + \sum_{i=1}^N (a_i + \sum_l b_{li} * m_l) * V_i \quad (3)$$

Table-2 lists the descriptive statistics of 82 subjects' anthropometric measurements. Among them are seven manual measurements collected in ANSUR II (Gordon et. al., 2014) and three derived ratio measurements.

## RESULTS AND CONCLUSIONS

First, we evaluated the accuracy of the reconstructed scalp curves from the first four and six loading vectors respectively by computing 3D point to point distance to the original curves. The mean error and standard deviation are summarized in Table-3. Using the first six loading vectors reduced the standard deviation. Hence the top six PC scores were used in the multiple variate linear regression (MLR) analysis and shape reconstruction.

Then we selected eight measurements: Head Length, Head Breadth, TrTOH, Menton-Sellion Length, Bizygomatic Breadth, Head Breadth to Head Length ratio, TrTOH to Head Breadth ratio and TrTOH to Head Length ratio as independent variables. Head Circumference was not used because that measurement is measured with a tape around hair which cannot reflect the true circumference of scalp.

Multiple variate linear regression (MLR) of the top six PC scores were performed. Table-4 displays the F-test results for the variable selections for PC0 ~ PC3 and the R-squared values from the MLR. We also tested MLR based on measurements selected by their F-test results (those  $p < 0.05$  are kept in fitting). The R-squared values from this set of MLR equations slightly decreased, so in the later computation we still used all eight measurements to predict PC scores.

**Table 1.** Description of observed shape variations of the feature curves.

PCA component	Sagittal plane view	Glabella plane view	Coronal plane view
PC0	Variation on the height and length of sagittal curves. Overall larger shape vs smaller shape	Length variation occurs at the front of head, which indicates a proportion change related to trasion location	Large variation on the height of coronal curves. Taller and wider vs shorter and narrower.
PC1	Length variation of the sagittal curves at the back of head	Length variation of the glabella curves at the back of head	Small variation in the breadth of coronal curve
PC2	Proportion change of trasion location combined with slightly length variation	Proportion change of trasion location combined with slightly length variation	Variation in breadth, maybe due to trasion location variation
PC3	Shorter in length and taller vs longer in length and shorter in height of sagittal section	The shape variation is mainly a scale factor in both section length and breadth, a longer and wider shape vs a shorter and narrower shape	Taller and narrower vs shorter and wider

**Table 2.** Descriptive statistics of the 10 anthropometric measurements utilized in this study.

	Min	Max	Mean	SD
Age (years)	19	56	35.9	9.03
Head Breadth (mm)	143	175	155.3	5.48
Head Length (mm)	187	224	201.0	6.53
Menton-Sellion Length (mm)	110	137	123.7	5.53
Bizygomatic Breadth (mm)	133	166	145.2	6.07
Head Circumference (mm)	545	615	575.9	15.15
Trasion to Top Of Head distance (TrTOH) (mm)	111	147	129.5	6.72
Ratio of head breadth and head length	0.6895	0.8426	0.7731	0.0317
Ratio of TrTOH to head breadth	0.7161	0.9459	0.8348	0.046
Ratio of TrTOH to head length	0.5441	0.7231	0.6446	0.0307

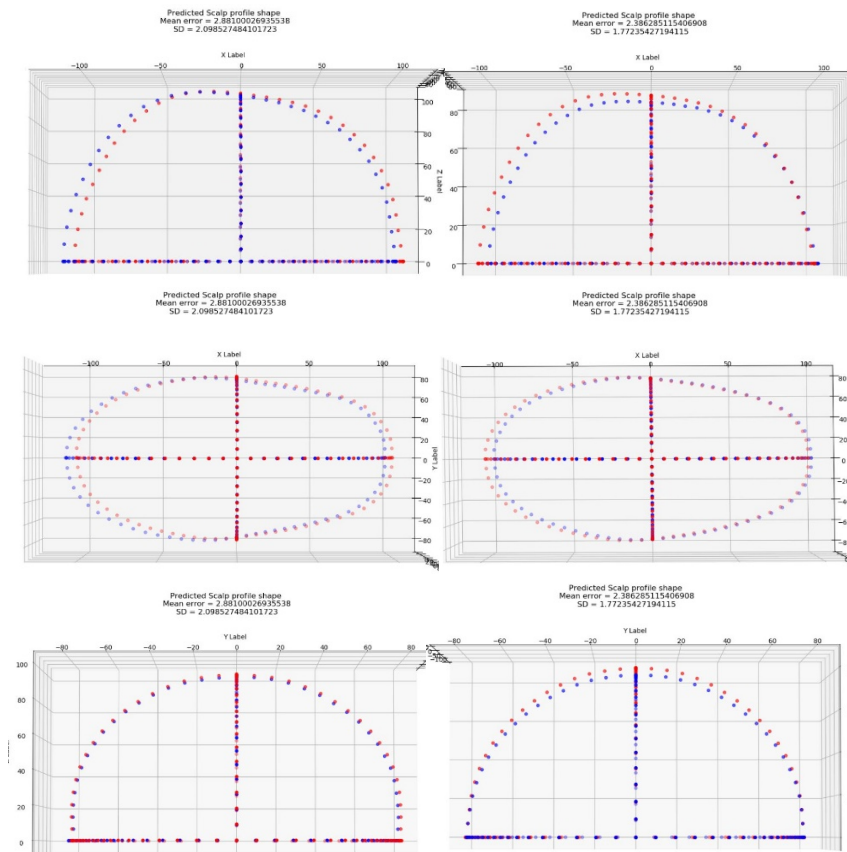
To evaluate the predicted scalp shape accuracy, we reconstructed the scalp shapes from the regression models with the eight measurements as inputs and then computed the distance between the corresponding points on the original scalp shape. The mean distance and standard deviation were recorded as a metric for the goodness of the prediction. We split the sample data into a training and a test group and perform a 10-fold cross-validation. That is, using regression models from training data (about 72 samples), we predicted scalp shapes that were not included in the training data for each batch (about eight samples) and rotated the split 10 times. When doing this, we received

**Table 3.** Reconstruction accuracy from top four and six loading vectors (unit=millimeter).

	Mean error	Standard deviation
Use loadings on PC0, PC1, PC2 and PC3	1.34	1.0139
Use loadings on PC0, PC1, PC2, PC3, PC4 and PC5	0.9633	0.7481

**Table 4.** F-test's p-value of MLR results from eight measurements on PC0 ~ PC3, shaded areas are those p-value > 0.05 and R-squared values for each MLR fitting.

	PC0 (R <sup>2</sup> =0.52017)	PC1 (R <sup>2</sup> =0.45398)	PC2 (R <sup>2</sup> =0.40173)	PC3 (R <sup>2</sup> =0.62526)
Head Length	4.3921e-04	8.9916e-08	2.1623e-02	4.7174e-03
Head Breadth	4.6515e-05	1.4548e-03	6.1504e-03	6.7737e-08
TrTOH	9.2066e-10	1.2127e-04	5.1006e-01	1.6591e-02
MentonSellion Length	9.7207e-01	2.3919e-05	1.2439e-01	6.0826e-01
Bizygomatic Breadth	6.6852e-02	2.4019e-03	2.436e-05	3.0671e-07
Breadth-Length-ratio	4.7383e-01	2.47e-01	2.1117e-05	3.481e-02
TrTOH-Breadth-ratio	5.4476e-03	1.3518e-01	2.2503e-02	4.0898e-09
TrTOH-Length-ratio	1.4384e-04	5.0047e-01	4.2380e-01	1.9455e-06

**Figure 4:** Two samples of predicted scalp shape from the measurements in Table-4 (blue = original shape, red = predicted shape).

an average mean distance error between the corresponding points of 2.8035 mm with an average standard deviation of 1.9654 mm from all tests. Figure 4 shows two examples that have mean errors of 2.88 and 2.39, respectively.

With a set of orthogonal feature curves it is possible to further derive a 3D shape of the scalp. The ultimate goal of this approach is to predict the scalp shape for head scans with hair in the ANSURII database. The 10-fold cross validation shows the mean distance error from MLR prediction is around 2.8 mm but there are some cases that the mean errors are larger than 5 mm. We will try different prediction methods to improve the accuracy and also continue to collect more bald scans to increase the size of the training data set. It's not clear if including facial scan as independent variables can improve prediction accuracy, but our experiment does show that using eight variables in Table-4 improved prediction accuracy over using less variables. Being able to reconstruct scalp's shape from traditional anthropometric measurements is important for leveraging existing 3D head surface scans to create complete head models for head-borne protective equipment designs.

## ACKNOWLEDGMENT

The author would like to thank Ms. Blake Mitchell for reviewing and suggestion to this paper.

## REFERENCES

- Bérar, M., Desvignes, M., Bailly, G., & Payan, Y. (2006). Statistical skull models from 3D X-ray images. *arXiv: Medical Physics*.
- Bérar, M, Tilotta, F, Glaunès, J., , Rozenholc, Y., (2011). Craniofacial reconstruction as a prediction problem using a Latent Root Regression model, *Forensic Science International*, Volume 210, Issues 1–3, 2011, Pages 228-236, ISSN 0379-0738, <https://doi.org/10.1016/j.forsciint.2011.03.010>.
- Dai, H., Pears, N., Duncan, C., (2017). Modelling of Orthogonal Craniofacial Profiles. *J. Imaging*, 3(4):55, 2017.
- Dai, H., Pears, N., Smith, W. et al. (2020). Statistical Modeling of Craniofacial Shape and Texture. *Int J Comput Vis* 128, 547–571. <https://doi.org/10.1007/s11263-019-01260-7>
- Ellena T, Skals S, Subic A, Mustafa H, Pang TY. (2017). 3D digital head form models of Australian cyclists. *Applied Ergonomics*. 2017 Mar;59(Pt A):11-18. DOI: 10.1016/j.apergo.2016.08.031. PMID: 27890118.
- Gordon, C.C., Blackwell, C.L., Bradtmiller B., Parham, J.L., Barrientos, P. Paquette, S.P., Corner, B.D., Carson, J.M., Venezia, J.C. Rockwell, B.M., Mucher, M, and Kristensen, S. (2014). 2010-2012 Anthropometric Survey of U.S. Army Personnel: Methods and Summary Statistics. Technical Report (Natick/TR-15/007). U.S. Army Natick Research, Development and Engineering Center, Natick, MA 01760-2646.
- Goto, L., Lee, W., Song, Y., Molenbroek, J., Goossens, R., (2015). Analysis of a 3D anthropometric data set of children for design applications. In: *Proceedings 19th Triennial Congress of the IEA*, vol. 9, p. 14.
- Green H, Curnoe D. (2009). Sexual dimorphism in southeast Asian crania: a geometric morphometric approach. *Homo*. 2009;60(6):517-534. doi:10.1016/j.jchb.2009.09.001

- Lacko D, Huysmans T, Parizel PM, De Bruyne G, Verwulgen S, Van Hulle MM, Sijbers J. (2015). Evaluation of an anthropometric shape model of the human scalp. *Appl Ergon.* 2015 May; 48:70-85. doi: 10.1016/j.apergo.2014.11.008. Epub 2014 Dec 6. PMID: 25683533.
- Lee, W., Goto, L., Molenbroek, J., Goossens, R., Wang, C., (2017). A Shape based Sizing System for Facial Wearable Product Design, Proceedings of 5th International Digital Human Modeling Symposium, Bonn, Germany 2017.
- Liu Y, Xi P, Joseph M, Zhuang Z, Shu C, Jiang L, Bergman M, Chen W. (2015). Variations in Head-and-Face Shape of Chinese Civilian Workers. *Ann Occup Hyg.* 2015 Aug;59(7):932-44. doi: 10.1093/annhyg/mev026. Epub 2015 Apr 9. PMID: 25858431; PMCID: PMC5504517.
- Park, B. K. D., Corner, B. D., Hudson, J. A., Whitestone, J., Mullenger, C. R., & Reed, M. P. (2021). A three-dimensional parametric adult head model with representation of scalp shape variability under hair. *Applied Ergonomics*, 90, 103239.
- Paysan, P., Lüthi, M., Albrecht, T., Lerch, A., Amberg, B., Santini, F., & Vetter, T. (2009). Face Reconstruction from Skull Shapes and Physical Attributes. In: Denzler J., Notni G., Süße H. (eds) *Pattern Recognition. DAGM 2009. Lecture Notes in Computer Science*, vol 5748. Springer, Berlin, Heidelberg
- Zhuang, Z., Shu, C., Xi, P., Bergmana, M., Joseph, M., (2013). Head-and-face shape variations of U.S. civilian workers, *Applied Ergonomics*, Volume 44, Issue 5, September 2013, Pages 775-784
- Zhuang, Z., Slice, D., Benson, S., Lynch, S., & Viscusi, D., (2010). Shape Analysis of 3D Head Scan Data for U.S. Respirator Users. *EURASIP J. Adv. Signal Process.* 2010, 248954. <https://doi.org/10.1155/2010/248954>